Development of ALE hydrodynamic code for laser-plasma interactions with self-generated magnetic fields

M. Kucharik[1], J. Limpouch[1], J. Nikl[1,2,3]

[1] *FNSPE, Czech Technical University in Prague, Prague, Czech Republic*

[2] *ELI-Beamlines, Institute of Physics, Czech Academy of Sciences, Prague, Czech Republic*

[3] *Institute of Plasma Physics, Czech Academy of Sciences, Prague, Czech Republic*

Abstract

Investigation of the laser-produced plasmas via hydrodynamic simulations belongs among popular tools allowing to design experimental setups with optimal parameters. Interpretation of complex processes which cannot be observed directly during experiments represents another field of application. Here, we present the application of the Arbitrary Lagrangian-Eulerian (ALE) framework in the context of laser-plasma simulations, which employs a computational mesh moving in a Lagrangian manner, i.e. naturally following the flow of the generated plasma. On the other hand, robustness of this approach under extreme conditions of laser/target interaction is guaranteed by a regular mesh improving mechanism followed by an accurate interpolation technique. In realistic simulations, additional physical models must be incorporated, such as accurate laser absorption, heat conductivity model, realistic equation of state, etc. In particular, we are mainly interested here in development of a magnetic field model in the context of full ALE algorithm, enabling to perform estimates of self-generated magnetic fields, when plasma density and temperature are not colinear.

Introduction

Many quantities of the laser produced plasma cannot be simply measured during experimental investigation, which makes the numerical simulations unavoidable for experiment interpretation and detailed insight into the processes during the interaction.

Two basic frameworks can be used in hydrodynamic simulations – Eulerian and Lagrangian. The classical Eulerian approach employs a static computational mesh, while a mesh moving with the fluid is used in the Lagrangian approach, making it well-suited for problems involving strong compressions or expansions typically present in laser/target simulations. However, the motion of the mesh can result in its degeneration in certain situations. For this reason, the arbitrary Lagrangian-Eulerian (ALE) method [1] has been developed, continuously improving the mesh by a rezoning method followed by a remapping step, transferring all fluid quantities conservatively to the rezoned mesh.

The 2D cylindrical Prague ALE (PALE) code [2] has been developed, incorporating the ALE algorithm with all necessary physics models (equations of state, models for heat conductivity, laser absorption, two-temperature fluid, etc). This code is used for simulations of a wide variety of problems, see for examples [3], [4], or [5]. Recently, the proposed model of spontaneously-generated magnetic fields based on the Biermann term discretization has been added, allowing to estimate the magnetic field distribution and magnitude in the interaction region.

Hydrodynamic Model

In the PALE code, we employ the compatible mimetic method [6] in the staggered discretization. The following set of Euler equations in the Lagrangian formulation is solved,

$$\frac{1}{\rho}\frac{d\rho}{dt} = -\vec{\nabla}\cdot\vec{w}, \quad \rho\frac{d\vec{w}}{dt} = -\vec{\nabla}\cdot p, \quad \rho\frac{d\varepsilon}{dt} = -p\vec{\nabla}\cdot\vec{w} - \vec{\nabla}\cdot(\kappa\vec{\nabla}T) - \vec{\nabla}\cdot\vec{I},$$

where the thermodynamic quantities (density ρ, pressure p, and specific internal energy ε) are located in the cell centers, and the fluid velocity $\vec{w}$ at the mesh nodes. The last two terms in the energy equation represent the heat exchange due to thermal conductivity and laser absorption, where T stands for fluid temperature, κ is the heat conductivity coefficient, and $\vec{I}$ represents the Poynting vector. For mesh rezoning, we employ the Winslow smoothing, followed by an approximate remapper with a posteriori repair [7] in the mesh sub-zones [8].

To approximate the source term representing absorption of the laser beam energy, the wave-based self-consistent model employing stationary solution of Maxwell equations [9] is employed. The parabolic heat-conductivity term is separated by the splitting technique [10] and solved by the mimetic support operators [11], while using the Spitzer-Harm κ coefficient and heat flux limiting. The QEOS equation of state [12] consistently interpolated by the HerEOS library [13] is used here. To approximate real laser geometry and avoid expensive 3D calculation, the axisymmetric $r-z$ cylindrical geometry is used.

The magnetic field generation is described by the Biermann battery term,

$$\frac{\mathrm{d}\vec{B}}{\mathrm{d}t} = -\nabla\times\vec{E} = -\frac{c}{e}\nabla\left(\frac{1}{n_e}\right)\times\nabla p_e,$$

where n_e is electron density and p_e electron pressure. The constants of electron charge e and speed of light c convert the generated field to the Gaussian units. Only the angular field component $\vec{B} = (0,0,B_\varphi)$ is considered here in the $r-z$ geometry. The derivatives of electron pressure and harmonic electron density are computed numerically using the least squares [14] approximation. In the remapping step of the ALE algorithm, B_φ is remapped in the form of magnetic energy density $b_\varphi = \frac{1}{\mu_0}B_\varphi^2$. Its reconstruction, integration, and repair is done similarly as the other cell-centered quantities, ensuring magnetic energy conservation to machine epsilon.

Numerical Examples

To verify the magnetic field generation model, a crossed-gradients test inspired by [15] was used. Density and electron temperature are set such that their gradients are perpendicular

$$\rho = 1 + 0.1\,(\cos(\pi r) + \cos(\pi\,(1-z))\,, \qquad T_e = 100 + 10\,(\cos(\pi r) + \cos(\pi z))\,,$$

leading to magnetic field generation in the center of the $\langle 0,1\rangle\,\mathrm{cm} \times \langle 0,1\rangle\,\mathrm{cm}$ domain. In this test, the hydrodynamic solver is disabled and only the magnetic field model is tested.

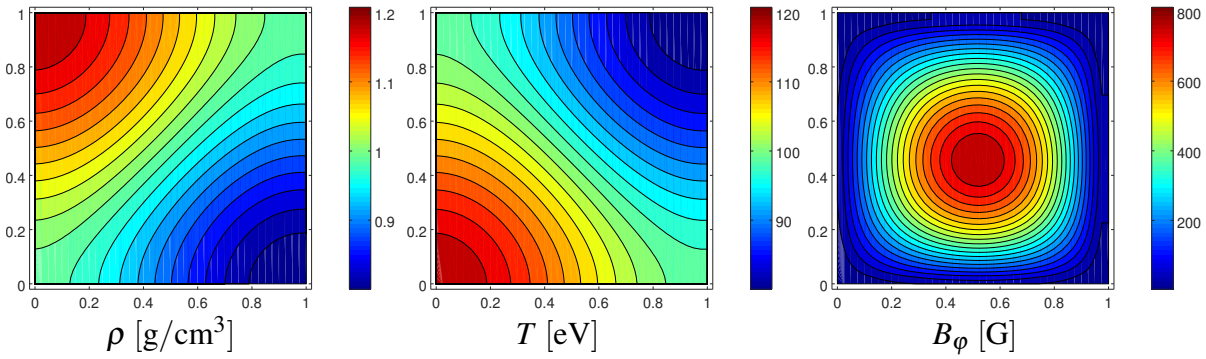

Figure 1: *Numerical profiles for the crossed-gradients test: mass density (left), temperature (central) and generated magnetic field (right) on* 40^2 *mesh at* $t = 200\,\mathrm{ns}$.

In Fig. 1, profiles of density, temperature, and generated magnetic field at $t = 200\,\mathrm{ns}$ on a 40^2 mesh are shown. The same test was run on a sequence of meshes in different resolutions. The analytic solution has been constructed and L_1 errors of the numerical values from the analytic ones have been computed, the results are presented in Tab. 1. The second order of convergence can be observed, and the model converges to the analytic profile.

n	L_1	order
10	$8.19 \cdot 10^{-2}$	
20	$2.20 \cdot 10^{-2}$	1.89
40	$5.60 \cdot 10^{-3}$	1.97
80	$1.41 \cdot 10^{-3}$	1.99
160	$3.53 \cdot 10^{-4}$	1.99
320	$1.03 \cdot 10^{-4}$	1.78

Table 1: L_1 *errors and orders of convergence of* B_φ *at* $t = 200\,\mathrm{ns}$ *on meshes with different resolutions.*

To demonstrate compatibility of the magnetic field model with the staggered ALE algorithm, a full test motivated by experiments at the PALS laser facility involving all available physics has been designed. A 500 J Gaussian pulse at 438 nm with spot radius 100 μm and FWHM length 400 ps irradiates a 20 μm thick Al foil, generates a shock wave melting and evaporating the material and producing plasma corona. The generated magnetic field at the time of pulse maximum in shown in Fig. 2. We can see a positive field behind the shown wave as well as a negative field in the low-density plasma. A relatively good agreement with the B_φ magnitude scaling law from [16] has been observed.

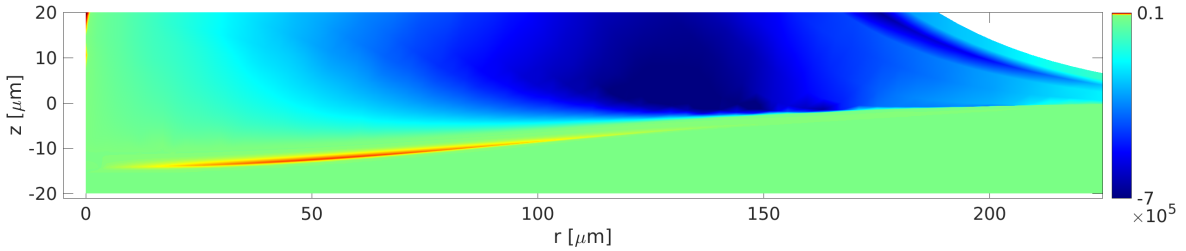

Figure 2: *Generated magnetic field* B_φ [G] *profile for the full test on* 100^2 *mesh at pulse maximum.*

Conclusions

The development of a magnetic field model and its integration to the PALE hydrodynamic code has been described and its validity demonstrated on typical realistic tests. In the near future, we plan to investigate the validity of the model in realistic simulations and extend it by incorporating the magnetic diffusion model. At the same time, a more advanced model based on curvilinear FEM discretization is being developed, for a preliminary report, see [17].

Acknowledgments

This work was supported by the Czech Science Foundation project 19-24619S, the European Regional Development Fund project CZ.02.1.01/0.0/0.0/16_019/0000778, the Czech Technical University grant SGS19/191/OHK4/3T/14, the EUROfusion project CfP-FSD-AWP21-ENR-01-CEA-02, and the Czech Ministry of Education project RVO 68407700. The results of the Project LQ1606 were obtained with the financial support of the Czech Ministry of Education, Youth and Sports as part of targeted support from the National Programme of Sustainability II.

References

[1] C. W. Hirt et al. *J. Comput. Phys.*, 14(3):227–253, 1974.

[2] R. Liska et al. In *FVCA, 4*, Springer Proceedings in Mathematics, pages 857–873. Springer, 2011.

[3] A. Picciotto et al. *Phys. Rev. X*, 4(3):031030, 2014.

[4] J. Badziak et al. *Laser Part. Beams*, 35:619–630, 2017.

[5] L. Giuffrida et al. *Phys. Rev. E*, 101(1):013204, 2020.

[6] E. J. Caramana et al. *J. Comput. Phys.*, 146(1):227–262, 1998.

[7] M. Kucharik at al. *J. Comput. Phys.*, 188(2):462–471, 2003.

[8] R. Loubere and M. Shashkov. *J. Comput. Phys.*, 209(1):105–138, 2005.

[9] J. Nikl et al. *Adv. Comput. Math.*, 45:1953–1976, 2019.

[10] R. Liska and M. Kucharik. In *Proceedings of EQUADIFF 11*, pages 213–222. STU, 2007.

[11] M. Shashkov and S. Steinberg. *J. Comput. Phys.*, 129(2):383–405, 1996.

[12] R. M. More et al. *Phys. Fluids*, 31(10):3059–3078, 1988.

[13] M. Zeman et al. *Comput. Math. Appl.*, 78(2):483–503, 2019.

[14] M. Kucharik and M. Shashkov. *J. Comput. Phys.*, 258:268–304, 2014.

[15] R. J. Kingham and A. R. Bell. *J. Comput. Phys.*, 194(1):1–34, 2004.

[16] S. Eliezer. *The Interaction of High-Power Lasers with Plasmas*. CRC Press, 2002.

[17] J. Nikl et al. In *WCCM-ECCOMAS2020, Scipedia*, 2021.